

# Crystalline and Transport Properties of Ga<sub>2</sub>Te<sub>3</sub> Synthesized by Metalorganic Chemical Vapor Deposition

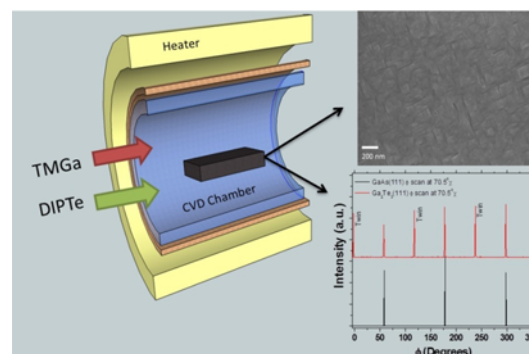
Peng-Yu Su, Sneha Banerjee, Rajendra Dahal, and Ishwara B. Bhat\*

Electrical, Computer and Systems Engineering Department, Rensselaer Polytechnic Institute,  
Troy, NY 12180, USA

(received date: 30 June 2015 / accepted date: 17 October 2015 / published date: 10 January 2016)

Ga<sub>2</sub>Te<sub>3</sub> films have been grown on GaAs(100) and (111) substrates using metalorganic chemical vapor deposition (MOCVD) at temperatures ranging from 350°C to 450°C. Very uniform films were grown at lower temperatures of 350°C on GaAs(100) substrates. As the temperature increased the roughness of the films increased, with many hillocks observed on films deposited at 450°C. The Ga<sub>2</sub>Te<sub>3</sub> films grown on GaAs(100) were determined to be single crystal by XRD characterization. On the other hand, XRD scans confirmed crystal twinning in the Ga<sub>2</sub>Te<sub>3</sub> films grown on GaAs(111) and the surface morphology also indicated the presence of twin grains. The films were determined to be *n*-type by hot-point probe testing. The carrier concentration could not be measured precisely as after photo-excitation, Ga<sub>2</sub>Te<sub>3</sub> exhibited the persistent photoconductivity (PPC) effect.

**Keywords:** metalorganic chemical vapor deposition, Ga<sub>2</sub>Te<sub>3</sub>, thermoelectric, crystal twinning



## 1. INTRODUCTION

Ga<sub>2</sub>Te<sub>3</sub> is one of the most studied defect semiconductors with a zinc-blende structure. Similar to other III<sub>2</sub>VI<sub>3</sub> materials, one third of the cation sites are vacant due to the non-stoichiometric structure. Over the years, Ga<sub>2</sub>Te<sub>3</sub> has emerged as a good candidate for thermoelectric devices because of its low thermal conductivity.<sup>[1,2]</sup> Kurosaki *et al.* confirmed the self-assembled 2-dimensional (2D) vacancy planes in Ga<sub>2</sub>Te<sub>3</sub> to be periodic with intervals of ~3.5 nm.<sup>[2]</sup> These self-assembled 2D planes are highly efficient at phonon scattering and thus reduce the thermal conductivity significantly. Cui *et al.* have reported Cu and Sb co-substitutions for Te in Ga<sub>2</sub>Te<sub>3</sub> which decrease the thermal conductivity and increase the electrical conductivity, making Ga<sub>2</sub>Te<sub>3</sub> a more promising candidate for thermoelectric

applications.<sup>[3]</sup> Ga<sub>2</sub>Te<sub>3</sub> has not only emerged as an excellent material for use in thermoelectric devices, but it also has the potential for application in phase change memory devices. As compared to traditional materials such as Ge<sub>2</sub>Sb<sub>2</sub>Te<sub>5</sub>, Ga<sub>2</sub>Te<sub>3</sub> has a higher bandgap and crystallization temperature and thus memory cells made with Ga<sub>2</sub>Te<sub>3</sub> have high switching speeds.<sup>[4]</sup>

To synthesize III<sub>2</sub>VI<sub>3</sub> materials, the furnace-alloyed technique is widely used for bulk Ga<sub>2</sub>Te<sub>3</sub>, In<sub>2</sub>Te<sub>3</sub> and Ga<sub>2</sub>Se<sub>3</sub>.<sup>[1-3,5]</sup> For thin film thermoelectric devices or memory devices, conventional semiconductor fabrication techniques are required. Ga<sub>2</sub>Se<sub>3</sub> and Ga<sub>2</sub>Te<sub>3</sub> have been grown epitaxially using molecular beam epitaxy (MBE).<sup>[6-8]</sup> Polycrystalline Ga<sub>2</sub>Se<sub>3</sub> and Ga<sub>2</sub>Te<sub>3</sub> have also been deposited by chemical vapor deposition (CVD), as reported by George *et al.*<sup>[9]</sup> In this work we report the epitaxial growth of Ga<sub>2</sub>Te<sub>3</sub> films on GaAs(100) and GaAs(111) substrates using metalorganic CVD (MOCVD). Surface morphology, crystallography and electrical properties of the Ga<sub>2</sub>Te<sub>3</sub> films grown by the above technique have also

\*Corresponding author: bhati@rpi.edu  
©KIM and Springer

been studied.

## 2. EXPERIMENTAL PROCEDURE

The  $\text{Ga}_2\text{Te}_3$  films were grown in a horizontal MOCVD reactor with a graphite susceptor and a hot-wall heating configuration. Semi-insulating GaAs(100) substrates with a misorientation of  $4^\circ$  towards  $(\bar{1}\bar{1}0)$  and nominal GaAs(111) wafers were used as the substrates. Before growth, GaAs substrates were cleaned with methanol to remove any organic impurities. This was followed by a 30 s dip in dilute HCl and subsequent rinsing with deionized water (DI water) and methanol. Trimethylgallium (TMGa) and Diisopropyltelluride (DIPTe) were used as the metalorganic sources for gallium and tellurium with ultra-high purity hydrogen (UHP  $\text{H}_2$ ) as the carrier gas. TMGa and DIPTe bubblers were maintained at  $5^\circ\text{C}$  and  $20^\circ\text{C}$ , respectively. The molar fractions of TMGa and DIPTe used were  $2.5 \times 10^{-4}$  and  $3.5 \times 10^{-4}$  respectively. The temperature of the susceptor was varied from  $350^\circ\text{C}$  to  $450^\circ\text{C}$ . Each growth was carried out at a pressure of 50 Torr with a total  $\text{H}_2$  flow of 1.1 standard liters per minute (SLM).

The film thickness was verified initially by Fourier transform infrared (FTIR) spectroscopy. Scanning electron microscopy (SEM) (Carl Zeiss Supra SEM 1550) was also used to verify the thickness from the cross-sectional view. SEM top view images were used to determine the surface morphology. The crystallography of  $\text{Ga}_2\text{Te}_3$  films was characterized using X-ray diffraction (XRD) (Bruker D8 Discover Diffractometer) with a Cu target. A Keithley 2400 source meter was used for current-voltage (I-V) measurements to determine the conductivity of the  $\text{Ga}_2\text{Te}_3$  films.

## 3. RESULTS AND DISCUSSION

Figures 1(a)-(c) show SEM top view images of  $\text{Ga}_2\text{Te}_3$  films grown at  $350^\circ\text{C}$ ,  $400^\circ\text{C}$ , and  $450^\circ\text{C}$ , respectively on GaAs(100) substrates. At a growth temperature of  $350^\circ\text{C}$ , the  $\text{Ga}_2\text{Te}_3$  film has a very smooth surface without hillocks or defects. The as-grown film surface was mirror-like when observed by the naked eye. When the growth temperature was increased to  $400^\circ\text{C}$ , inverse pyramid-like defects were observed. The four facets of the inverse-pyramid-like defects are the four  $\{111\}$  surfaces due to the lower growth rate of (111) oriented  $\text{Ga}_2\text{Te}_3$ . The depth of the defects was 50 - 100 nm with a total  $\text{Ga}_2\text{Te}_3$  film thickness of 600 nm. With the growth temperature of  $450^\circ\text{C}$ , the surface became very rough with sharp hillocks and defects and the  $\{111\}$  facets dominated the surface. Some of the valleys are as deep as 250 nm to 300 nm with a total film thickness of  $\sim 750$  nm, as shown in Fig. 2.

The SEM top view images of  $\text{Ga}_2\text{Te}_3$  film grown on GaAs(111) substrates at  $350^\circ\text{C}$ ,  $400^\circ\text{C}$  and  $450^\circ\text{C}$  are shown in Figs. 3(a)-(c). It is evident from the figures that with

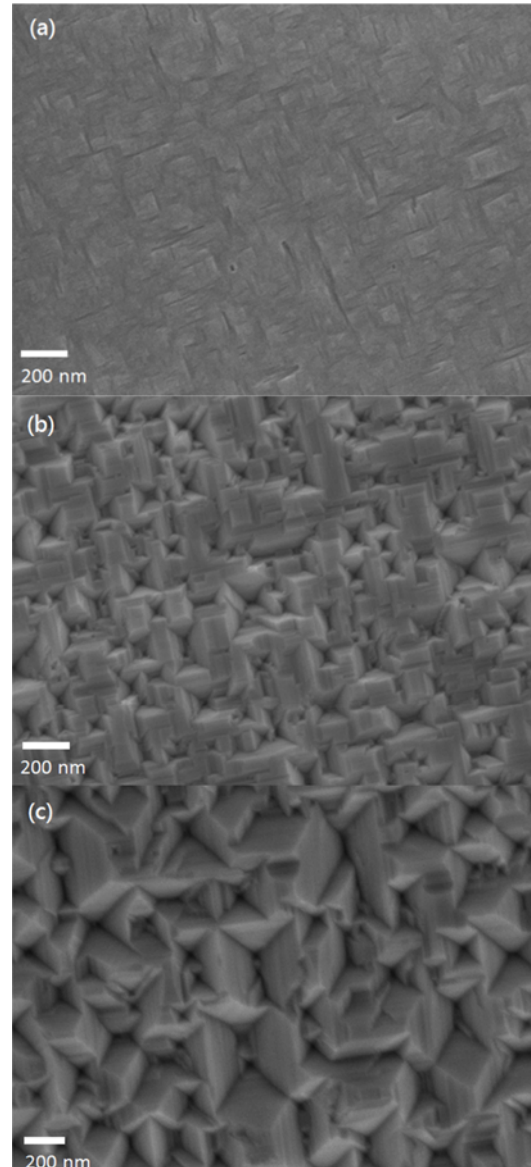


**Fig. 1.** SEM top view images showing the surface morphology of  $\text{Ga}_2\text{Te}_3$  films grown on GaAs (100) substrate at (a)  $350^\circ\text{C}$ , (b)  $400^\circ\text{C}$  and (c)  $450^\circ\text{C}$ .

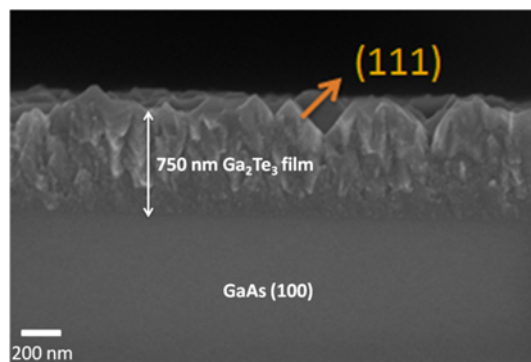


**Fig. 2.** SEM cross-sectional image showing the thickness and unevenness of the  $\text{Ga}_2\text{Te}_3$  film grown on GaAs (100) at  $450^\circ\text{C}$ .

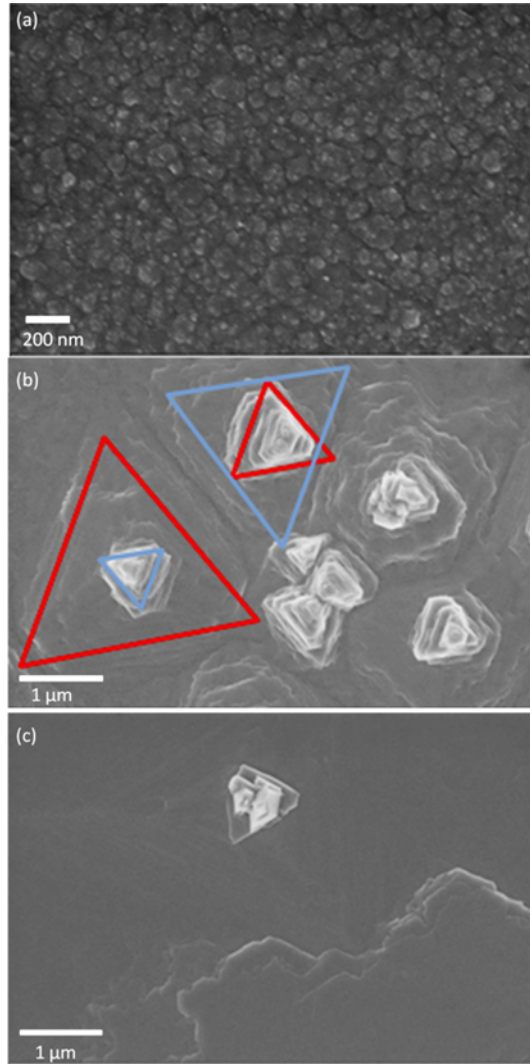


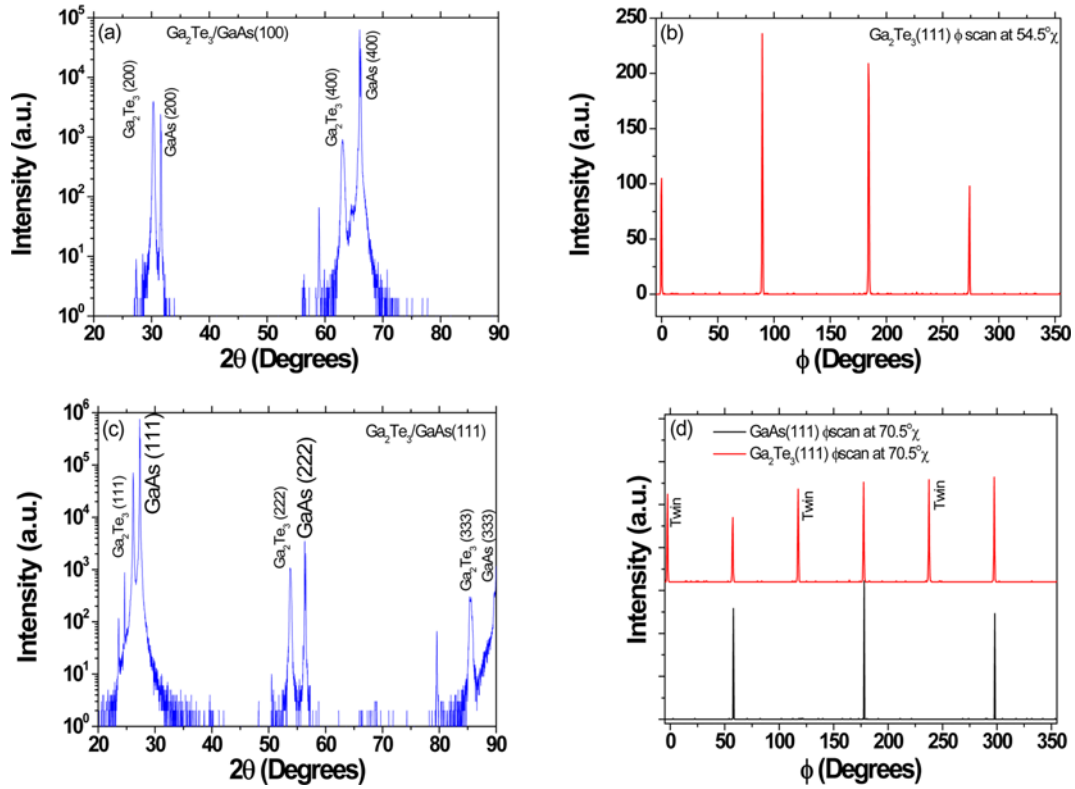
**Fig. 3.** SEM top view images showing the surface morphology of  $\text{Ga}_2\text{Te}_3$  films grown on GaAs (111) substrate at (a) 350°C, (b) 400°C, and (c) 450°C.

increasing growth temperatures from 350°C to 450°C, the grain sizes increase from  $\sim 200$  nm to  $\sim 1.5$   $\mu\text{m}$ . In addition, the triangular grain domains are rotated by  $60^\circ$  with respect to each other. Therefore, twin defects are expected in the  $\text{Ga}_2\text{Te}_3$  growth on GaAs (111) substrates. XRD in-plane rotation  $\varphi$  scans support the presence of crystal twinning which will be revealed shortly. The twinning of the  $\text{Ga}_2\text{Te}_3$  crystal happens not only at the GaAs/ $\text{Ga}_2\text{Te}_3$  interface, but also takes place during the growth of the film. This can be seen in Fig. 3(b), where the upper grains are rotated with respect to the base grains (marked by the red and blue triangles, respectively). As reported in the literature, bulk  $\text{Ga}_2\text{Te}_3$  can have self-assembled or randomly distributed vacancy planes.<sup>[2,5]</sup> Such defects determine the physical properties of the material. These defects and their response to annealing will be studied in detail in the future.

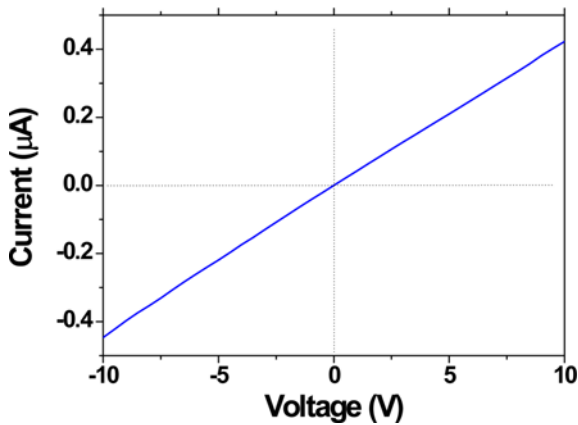
Although the surface morphology of  $\text{Ga}_2\text{Te}_3$  films depends significantly on the growth temperature, the films' crystalline properties varied little in the growth temperature range of 350°C to 450°C. Figure 4(a) shows the  $\theta$ - $2\theta$  scan of the  $\text{Ga}_2\text{Te}_3$  film grown at 450°C on GaAs(100). Apart from GaAs substrate peaks,  $\text{Ga}_2\text{Te}_3(200)$  and  $\text{Ga}_2\text{Te}_3(400)$  peaks were observed at  $2\theta = 30.28^\circ$  and  $62.99^\circ$ , respectively. The peak positions indicate the zincblende structure of  $\text{Ga}_2\text{Te}_3$  with a lattice constant of  $\sim 5.9$  Å and also point out the  $\langle 100 \rangle$  out of plane growth direction. Peaks associated with other Ga and Te compounds (for example, GaTe and  $\text{Ga}_2\text{Te}_5$ ) were not observed here. To verify that the thin film  $\text{Ga}_2\text{Te}_3$  was single crystalline and not of biaxial or fiber texture, XRD in-plane rotation  $\varphi$  scan of  $\text{Ga}_2\text{Te}_3$  were taken and are shown in Fig. 4(b). The  $\theta$  and  $2\theta$  angles were first set to  $13.075^\circ$  and  $26.15^\circ$ , respectively to satisfy the Bragg diffraction condition for  $\text{Ga}_2\text{Te}_3$  {111} planes. The  $\chi$  angle was set to  $54.5^\circ$ , the angle between the  $\langle 100 \rangle$  out of plane direction and  $\langle 111 \rangle$ . From the XRD  $\varphi$  scan, the 4 sharp {111} peaks with  $90^\circ$  separations indicate that single crystal  $\text{Ga}_2\text{Te}_3(100)$  films were grown on GaAs(100) substrates. N. Teraguchi *et al.* have reported that a growth temperature of 400°C was required to grow  $\text{Ga}_2\text{Te}_3$  on InP by MBE.<sup>[8]</sup> However, they were unsuccessful in growing  $\text{Ga}_2\text{Te}_3$  on GaAs substrates probably due to the lattice mismatch. By using the MOCVD technique, with growth temperatures varying from 350°C to 450°C, single crystal  $\text{Ga}_2\text{Te}_3$  has been grown on GaAs(100) substrates successfully.

Figure 4(c) shows the XRD  $\theta$ - $2\theta$  scan of the  $\text{Ga}_2\text{Te}_3$  film grown at 450°C on GaAs(111). Similar to the  $\text{Ga}_2\text{Te}_3$  growth on GaAs(100) substrates, only GaAs and  $\text{Ga}_2\text{Te}_3$  (111), (222) and (333) peaks could be observed. Other Ga and Te compound peaks were not observed. To further characterize the crystalline properties, XRD in-plane rotation  $\varphi$  scans of  $\text{Ga}_2\text{Te}_3(111)$  and GaAs(111) at  $\chi = 70.5^\circ$  are shown in Fig. 4(d). Three GaAs{111} peaks with  $120^\circ$  separations were observed in the  $\varphi$  scan, demonstrating the single crystal nature of the GaAs substrate. However, instead of three peaks, six  $\text{Ga}_2\text{Te}_3\{111\}$  peaks with  $60^\circ$  separations were observed in XRD  $\varphi$  scan. The observed six-fold symmetry is due to twin domains; three  $\text{Ga}_2\text{Te}_3\{111\}$  twin peaks show up at the midpoints of  $\text{Ga}_2\text{Te}_3$  {111} peaks. Since both zincblende (111) and wurtzite(0001) orientations are polarized and hexagonal close-packed, crystal twinning occurs quite often during crystal growth of zincblende materials due to the insertion of a monolayer of a wurtzite(0001) surface. The presence of crystal twinning has been observed in several other zincblende materials such as CdTe and GaAs.<sup>[10,11]</sup>

Figure 5 shows the dark I-V characteristics obtained upon probing the  $\text{Ga}_2\text{Te}_3$  film grown on semi-insulating GaAs(100). Indium pellets were melted and deposited at two corners of the sample to serve as the contacts. Good ohmic contact was formed, as evident from Fig. 5. A hot-point probe test



**Fig. 4.** XRD (a)  $\theta$ - $2\theta$  scan of  $\text{Ga}_2\text{Te}_3$  film grown at  $450^\circ\text{C}$  on GaAs (100) substrate, (b) In-plane rotation  $\phi$  scan of  $\text{Ga}_2\text{Te}_3$ ; setting  $\theta$  and  $2\theta$  angles to  $13.075^\circ$  and  $26.15^\circ$  and  $\chi$  to  $54.5^\circ$ , (c)  $\theta$ - $2\theta$  scan of  $\text{Ga}_2\text{Te}_3$  film grown at  $450^\circ\text{C}$  on GaAs (111) substrate, and (d) In-plane rotation  $\phi$  scans of  $\text{Ga}_2\text{Te}_3$  (111) and GaAs (111) at  $\chi = 70.5^\circ$ .



**Fig. 5.** The dark I-V characteristics obtained on probing the  $\text{Ga}_2\text{Te}_3$  film grown on semi-insulating GaAs (100).

conducted on the same sample determined it to be *n*-type. The sample was illuminated and the light current measured. After removal of the light excitation, the I-V curve did not correspond to the dark I-V curve obtained earlier. A couple of readings were taken successively with different results each time. Also, measurements of carrier concentration and

mobility by Hall testing gave inconsistent results. This effect was concluded to be due to the persistent photoconductivity (PPC) effect.<sup>[12]</sup> This effect is observed in many semiconductor materials and configurations, including thin film semiconductors due to the presence of deep level centers and defects. The photoconductivity which persists long after the removal of photoexcitation results in a variation in carrier concentration with time.

#### 4. CONCLUSIONS

In summary, it was shown that single crystal  $\text{Ga}_2\text{Te}_3$  can be grown on a GaAs(100) substrate. On GaAs(111) substrates, however, crystal twinning was observed. XRD characterization was used to arrive at the aforementioned conclusions. A very uniform film was obtained on GaAs(100) at the lower end of the temperature range ( $350^\circ\text{C}$ ) used for the growth. The non-uniformity of the film increased at higher growth temperatures, though the crystallographic orientation remained the same. For films grown on GaAs(111) the grain sizes increased with increasing susceptor temperature. The as-grown  $\text{Ga}_2\text{Te}_3$  films were determined to be *n*-type and indium was used to form good ohmic contact.

## ACKNOWLEDGEMENTS

The authors want to thank Dr. H. R. Vydyanath of IRDT Solutions for the many discussions and main motivations for this work. This material is based upon the work supported by the MDA under Contract No. HQ0147-13-C-7186.

## REFERENCES

1. S. Yamanaka, M. Ishimaru, A. Charoenphakdee, H. Matsumoto, and K. Kurosaki, *J. Electron. Mater.* **38**, 1392 (2009).
2. K. Kurosaki, H. Matsumoto, A. Charoenphakdee, S. Yamanaka, M. Ishimaru, and Y. Hirotsu, *Appl. Phys. Lett.* **93**, 012101 (2008).
3. J. Cui, Y. Gao, H. Zhou, Y. Li, Q. Meng, and J. Yang, *Appl. Phys. Lett.* **101**, 081908 (2012).
4. H. Zhu, J. Yin, Y. Xia, and Z. Liu, *Appl. Phys. Lett.* **97**, 083504 (2010).
5. C.-E. Kim, K. Kurosaki, M. Ishimaru, H. Muta, and S. Yamanaka, *J. Electron. Mater.* **40**, 999 (2011).
6. D. Lis, Y. Nakamura, N. Otsuka, J. Qiu, M. Kobayashi, and R. L. Gunshor, *J. Vac. Sci. Technol. B* **9**, 2167 (1991).
7. N. Teraguchi, M. Konagai, F. Kato, and K. Takahashi, *J. Crystal Growth* **115**, 798 (1991).
8. N. Teraguchi, F. Kato, M. Konagai, and K. Takahashi, *Jpn. J. Appl. Phys.* **28**, L2134 (1989).
9. K. George, C. H. (Kees) de Groot, C. Gurnani, A. L. Hector, R. Huang, M. Jura, W. Levason, and G. Reid, *Chem. Mater.* **25**, 1829 (2013).
10. Y. P. Chen, J. P. Faurie, S. Sivananthan, G. C. Hua, and N. Otsuka, *J. Electron. Mater.* **24**, 475 (1995).
11. Y. Park, M. J. Cich, R. Zhao, P. Specht, E. R. Weber, E. Stach, and S. Nozaki, *J. Vac. Sci. Technol. B* **18**, 1566 (2000).
12. H. X. Jiang, G. Brown, and J. Y. Lin, *J. Appl. Phys.* **69**, 6701 (1991).